Available online at www.sciencedirect.com
SCIENCE DIRECT®
Chemical Physics Letters 397 (2004) 417–421
CHEMICAL PHYSICS LETTERS
www.elsevier.com/locate/cplett

Globally cohesive drops without interfacial tension

Ludwig C. Nitsche [a,*], Anh Nguyen [b], Geoffrey Evans [b]

[a] Department of Chemical Engineering, University of Illinois at Chicago, 810 South Clinton Street, Chicago, IL 60607, USA
[b] Department of Chemical Engineering, University of Newcastle, University Drive, Callaghan, NSW 2038, Australia

Received 3 May 2004; in final form 2 September 2004

Abstract

For sedimenting, immiscible drops at unit viscosity ratio, a cohesive chemical potential is formulated to agree formally with the boundary-integral (BI) equation of Stokes flow. Against conventional wisdom, the resulting 'bulk cohesion' (BC) force field does *not* give rise to interfacial tension. Nevertheless, particle simulations based upon this concept accurately reproduce complex shape evolutions of trailing drops as calculated with BI. The BC force is easier to compute than volumetric versions of interfacial tension, and the radius of cohesion need not be small.

1. Bulk cohesion versus interfacial tension

Cohesion between molecules in a liquid phase enters the continuum equations of fluid dynamics *indirectly*, through the phenomenon and concept of surface (or interfacial) tension. Straightforward descriptions of surface energy [1–3] belie the subtlety of arguments needed to explain the origin of *tangential tension* at the surface, and of its mescoscale equivalent: negative surface-excess pressure [4]. The explanation involves anisotropic fall-off of the time-averaged, summed intermolecular forces near the surface [5].

In order to track very complicated interfacial deformations (coalescence and rupture), computational methods in continuum fluid dynamics usually take a volumetric tack [6–16], whereby the tensile forces are smeared out over a thin but finite 'active' layer straddling the mathematical surface on which the stress-jump boundary condition would otherwise be imposed. In this static continuum picture (Fig. 1a), which does not explicitly acknowledge the dynamic equilibrium between attractive and repulsive intermolecular forces, mutual attraction between only those material points lying within the thin surface layer produces the defining, anisotropic property of interfacial tension: the resulting normal force is always directed toward the concave side of the interface. Thus it points toward or away from the drop, according to the sign of the local surface mean curvature H.

A more superficial picture, involving isotropic attraction between *all* molecules or material points within a certain radius of cohesion (Fig. 1b), is consistent with the typical textbook explanation of surface energy [1–3]. But this model fails entirely to provide a mechanism for surface tension [5], because the resultant of unbalanced cohesive forces always points back into the drop phase, no matter what the curvature of the surface. It was probably the misapplication of this conceptual picture at the molecular scale that led to early controversies about the origin, and even the actual existence, of surface tension [5]. We shall refer to such volumetric forces as representing 'bulk cohesion' (BC), to distinguish them very clearly from the forces (Fig. 1a) that actually produce interfacial tension (IT).

* Corresponding author. Fax: +1 312 996 0808.
E-mail addresses: lcn@uic.edu (L.C. Nitsche), anh.nguyen@newcastle.edu.au (A. Nguyen), geoffrey.evans@newcastle.edu.au (G. Evans).

0009-2614/$ - see front matter © 2004 Elsevier B.V. All rights reserved.
doi:10.1016/j.cplett.2004.09.006

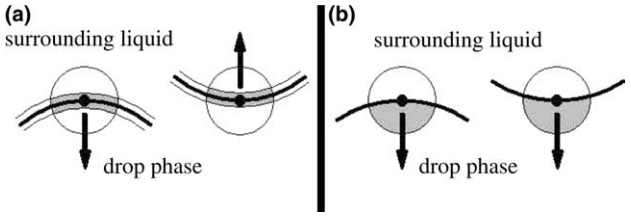

Fig. 1. Two stylized, continuum views of molecular cohesion and the resultant normal force at the surface. Self-cohesion occurs within the shaded areas, and the circles indicate the radius of attraction: (a) interfacial tension (IT), (b) bulk cohesion (BC).

Heretofore, volume-based computation in fluid dynamics has had to overcome the numerical burdens associated with IT forces: capturing interfaces and resolving surface mean curvature accurately from volumetric information [6–16]. Obviously, surfaces will also contract in response to bulk cohesion – despite its failure to produce interfacial tension. What seems to remain unexploited in the long history of numerical fluid dynamics is the observation that the BC force can be *quantitatively* accurate in predicting complicated behaviors of immiscible drops – *even when the range of cohesion is not small compared to the dimension of the drop(s)*. The following theoretical derivation and numerical example will justify this conclusion with reference to gravity-driven flows of drops of the same viscosity as the surrounding liquid.

2. Chemical potential for bulk cohesion

The volumetric force field that animates flow is given by the gradient of a general chemical potential, which involves gravitational and cohesive contributions:

$$\mathbf{f}_{\mathrm{BC}}(\mathbf{r}) = \beta\hat{\mathbf{g}} + \alpha\nabla \ln[c(\mathbf{r})]. \tag{1}$$

Here $\hat{\mathbf{g}}$ is the unit vector pointing in the direction of gravity, and α and β are parameters (related to the density, viscosity and interfacial tension) that will be determined below. The concentration field $c(\mathbf{r})$ of the drop(s) is the phase (or color) function, which is constant (say, unity) inside the drop(s), vanishes outside, and has a sharp discontinuity along the interface. The force field $\mathbf{f}_{\mathrm{BC}}(\mathbf{r})$ can be interpreted as a generalized function, or else the pointwise concentration field $c(\mathbf{r})$ in Eq. (1) can be replaced with a smoothed concentration field (in order that $\nabla c(\mathbf{r})$ is defined in the ordinary sense when $\mathbf{r}$ lies on the interface):

$$\bar{c}(\mathbf{r}) = \left[4\pi I_2 \epsilon^3\right]^{-1} \int\int\int_{V_\infty} c(\mathbf{q})\phi(\|\mathbf{r}-\mathbf{q}\|/\epsilon)\, \mathrm{d}^3 q \tag{2}$$

with $\phi(x) = 0$ for $x>1$ and

$$I_n = \int_0^1 \phi(x) x^n \, \mathrm{d}x. \tag{3}$$

The dimensionless weight function ϕ plays the role of a cohesive potential, which acts over a radius ϵ that is accessible to the continuum view. There is considerable latitude as to the functional form of ϕ: the radial integrals I_2 and I_3 automatically extract its dynamically significant features. For the particle simulations reported below, we used a smooth function based upon a solution of the radial Helmholtz equation,

$$\phi(x) = (2\sin(\pi x) + \sin(2\pi x))/(2\pi x). \tag{4}$$

The bulk cohesion force is nonzero only for drop-phase material points lying within distance ϵ of the surface, and it always points from the surrounding liquid back into the drop(s).

$$\mathbf{f}_{\mathrm{BC}} \approx -(\alpha/\epsilon)(I_1/I_2)\mathbf{n}, \quad \mathbf{r} \in S_{\mathrm{drop}} \tag{5}$$

with $\mathbf{n}$ the outward pointing unit normal vector. That means cohesion *without any interfacial tension.*

To examine how and why the IT and BC forces, which differ qualitatively (Fig. 1), can give rise to quantitatively similar velocity fields and observable dynamics, we must relate $\mathbf{f}_{\mathrm{BC}}$ to the usual interfacial stress-jump boundary condition. In the process we will change a previous proposal [17] for the form of BC forces in a subtle but very crucial way.

3. Transferring surface mean curvature to the volume

Subsequent arguments will rely on a Green's-function representation of the velocity field, which restricts the considerations to creeping flows of drops that have the same viscosity as the surrounding liquid. As will be seen below, interesting phenomena persist within these simplifying assumptions. The average concentration $\bar{c}(\mathbf{r})$ is exactly 1/2 when it is evaluated at a material point $\mathbf{r}$ lying on a flat interface. If the interface is curved, then the surface point $\mathbf{r}$ is slightly more or less than half surrounded by nearby material points of the drop phase, according to the local surface mean curvature $H(\mathbf{r})$, and $\bar{c}(\mathbf{r})$ differs slightly from 1/2:

$$\bar{c} = \frac{1}{2}\left\{1 - \left(\frac{1}{2}\frac{I_3}{I_2}\right)(H\epsilon) - \left(\frac{A}{16}\frac{I_5}{I_2}\right)(H\epsilon)^3 + \mathrm{O}(\epsilon^5)\right\}, \tag{6}$$

$$= \frac{1}{2}\left\{\exp\left[-\left(\frac{1}{2}\frac{I_3}{I_2}\right)(H\epsilon)\right] - \frac{1}{8}\left(\frac{I_3}{I_2}\right)^2 (H\epsilon)^2 + \mathrm{O}(\epsilon^3)\right\}. \tag{7}$$

The coefficient A is given in terms of $H(\mathbf{r})$, the Guassian curvature $K(\mathbf{r})$, and a function $f(\xi,\psi)$ that specifies the surface as a Monge patch [18], with ξ and ψ the local Cartesian coordinates in the tangent plane:

$$A = \frac{3K}{H^2} - 5 + \frac{\nabla^4 f}{4H^3}. \tag{8}$$

Formally, the truncated expansions (6) and (7) require $H\epsilon \ll 1$. But the constants in the expansion conspire to relax this restriction considerably in numerical practice.

Retaining only the linear term on the RHS of Eq. (6) represents a purely geometric approximation, which has been observed numerically to yield surprisingly accurate results for a prolate spheroid (transverse/longitudinal axis ratio $R = 0.6$) with ϵ on the order of H^{-1} [17]. From the next term in the expansion we can now see why this was so. At the tips of the spheroid (at which the curvature is the highest and the error is the biggest) we have

$$\left|\frac{\text{3rd term}}{\text{2nd term}}\right| = \left|\frac{AI_5}{8I_3}\right|(H\epsilon)^2 = (0.0746)|R^2 - 1|(H\epsilon)^2. \quad (9)$$

Although this result uses I_3 and I_5 based upon the particular functional form (4) for the cohesive potential ϕ, similar shapes yield a similarly forgiving asymptotic expansion.

The further approximation (7) enables us to write the mean curvature in terms of the cohesive chemical potential:

$$H \approx -\frac{2}{\epsilon}\frac{I_2}{I_3}(\ln \bar{c} + \ln 2). \quad (10)$$

This physically essential truncation is justified by noting the coefficient of $(H\epsilon)$ in the relative error: $I_3/4I_2 = 0.115$.

For unit viscosity ratio, the (dimensionless) boundary-integral (BI) equation for Stokes flow [19–26] reduces to a superposition of point forces over the interface to yield the velocity field directly:

$$\mathbf{v}(\mathbf{r}) = \int\int_{S_{\text{drop}}} [Bo(\hat{\mathbf{g}}\cdot\mathbf{q}) - 2H(\mathbf{q})]\mathbf{n}(\mathbf{q})\cdot G(\mathbf{q}-\mathbf{r})\,\mathrm{d}^2q \quad (11)$$

with Bo the Bond number and $G(\mathbf{r})$ the Stokeslet or Oseen–Burgers tensor,

$$G(\mathbf{r}) = \frac{1}{8\pi}\left[r^{-1}\mathbf{I} + r^{-3}\mathbf{rr}\right]. \quad (12)$$

In Eq. (11) the mean curvature term represents interfacial tension (Fig. 1a), and the action of gravity has been transferred artificially from the volume of the drop to its interface.

Substituting Eq. (10) for H, and using the solenoidal nature of the Stokeslet tensor, one obtains

$$\mathbf{v}(\mathbf{r}) \approx \int\int_{S_{\text{drop}}} \left[Bo(\hat{\mathbf{g}}\cdot\mathbf{q}) + \frac{4}{\epsilon}\frac{I_2}{I_3}\ln\bar{c}(\mathbf{q})\right]\mathbf{n}(\mathbf{q})\cdot G(\mathbf{q}-\mathbf{r})\,\mathrm{d}^2q. \quad (13)$$

When we use the divergence theorem to transfer the surface integral to the volume of the drop, we recover the Green's-function solution of the inhomogeneous Stokes equations, where the volumetric force has precisely the thermodynamic form of Eq. (1), with $\beta = Bo$ and $\alpha = (4/\epsilon)(I_2/I_3)$:

$$\mathbf{v}(\mathbf{r}) \approx \int\int\int_{V_{\text{drop}}} \mathbf{f}_{\text{BC}}(\mathbf{q})\cdot G(\mathbf{r}-\mathbf{q})\,\mathrm{d}^3q. \quad (14)$$

For any value of the interfacial tension (which enters the dimensionless Bond number), the corresponding coefficient α of bulk cohesion is determined by the above derivation, and should *not* be regarded as an empirically adjusted parameter. Eq. (14) justifies us in regarding $\mathbf{f}_{\text{BC}}(\mathbf{r})$ as the gravitational–cohesive force field that drives Stokes flow, at least in the case of unit viscosity ratio. Thus, volumizing the tensile force at the interface has produced a non-IT force field (bulk cohesion) that drives essentially the same velocity field.

4. Simulation of sedimenting immiscible drops: BC versus IT

The BC force (1), (2) could be applied in any volumetric CFD method [6–16]. Our previous papers [27,17] have addressed one advantageous avenue of computational implementation: using a swarm of discrete particles, which are convected by the flow field that the particles themselves generate through a summed Monte-Carlo approximation of the volume integral (14).

For the newer simulation shown in Fig. 2, which involves *many* more particles than before, the summations are reduced by lumping particles together into cells [28], as indicated by the superimposed grids, and using a second-order multipole expansion for each cell. (Near-cell interactions are, however, summed directly over the particles.) The singular Green's function (12) is also regularized by smearing it out over a range of twice the mean particle spacing; cf. [29,30]. The resulting 'fuzzy' Stokeslets overlap each other's clouds of force.

A particularly stringent test of the BC force is provided by a comparison with the boundary-integral method, because the latter concentrates *all* of the hydrodynamic information on the surface, and implements interfacial tension directly; cf. Eq. (11). In Fig. 2 the BI calculations of Davis [25] for two buoyant drops ($Bo = 5$) are compared with our particle-swarm implementation of Eq. (14). Here bulk cohesion is truly global, as $\epsilon = 1$ coincides with the radius of the initially spherical drops. Nevertheless, the shapes of both drops are accurately resolved, and the vertical shift in Fig. 2d amounts to only 4% of the cumulative distance traveled. Because the radius of cohesion vastly exceeds the gap between the drops, immediate (unphysical) coalescence of the drops must be prevented by artificial means: the particles are divided into two different 'species', which cohere within the same drop, but do not interact with particles making up the other drop [31].

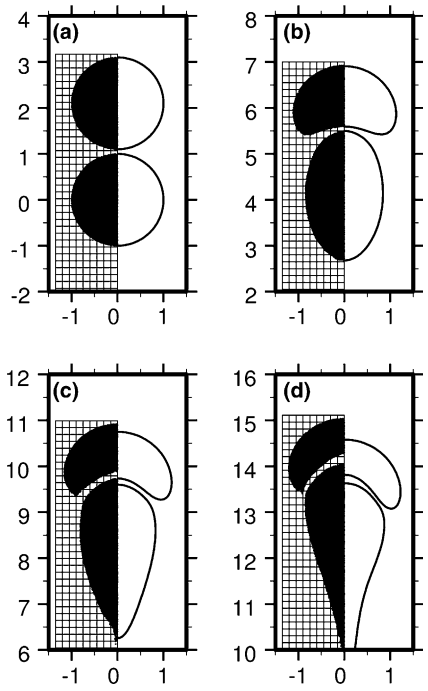

Fig. 2. Shape evolution of two buoyant drops ($Bo = 5$) of the same viscosity as the surrounding liquid. Referred to the dimensionless basis of Eq. (11), both drops start out as unit spheres, separated by a gap of 1/10. In each graph the drop outline appearing on the right half corresponds to the axisymmetric BI calculations of Davis [25]. The left half shows a meridional slice of two swarms totalling 425,625 fuzzy Stokeslets, with a global radius of cohesion ($\epsilon = 1$) for $\mathbf{f}_{BC}$. Cohesion *between* the two drops is suppressed to avoid unphysically premature coalescence: (a) $t = 0$; (b) $t = 2$; (c) $t = 4$; (d) $t = 6$.

5. Conclusions

The main conclusion of the above work is that interfacial tension need not be invoked to explain the gravity-driven motion and deformation of immiscible drops. Isotropic bulk cohesion (Fig. 1b) produces essentially the same velocity fields and resultant shape evolutions, in the case of unit viscosity ratio. Only the attendant pressure fields (which obviously differ) can distinguish between the two mechanisms. Even when the BC driving force acts over a global range, dynamics based upon it adequately mimmick relatively fine features of drop shapes. The BC force is simpler to calculate than volumetric formulations of interfacial tension [6–16].

A subtle but very crucial role is played by the approximation (7). It is this step that ties the surface mean curvature H to the thermodynamic form (1) of the cohesive potential. Arguing from Eq. (6) alone, one would arrive at a cohesive force of the form

$$\mathbf{f}(\mathbf{r}) = \left(\frac{8}{\epsilon}\frac{I_2}{I_3}\right)\nabla\bar{c}. \tag{15}$$

In earlier work [17], the inaccuracies associated with such a formulation had inadvertently been obscured by averaging of the resultant particle forces. Improvements in accuracy of the particle simulations (described above) reveal the chemical potential form of Eq. (1) to be the correct one.

Eq. (1) would have the form of a diffusional driving force if the coefficient α were negative. The diffusive flux would then be directly proportional to $\mathbf{f}_{BC}$, in contrast to the convolution integral (14) that produces the convective flux of Stokes flow. Thus, diffusion and creeping flow are produced by the same type of thermodynamic driving force, acting through different propagators.

Acknowledgements

The authors are grateful for the BI code [25] generously provided by Professor Robert H. Davis, University of Colorado, Boulder, which enabled the comparison in Fig. 2. Thanks are also due to Professor Constantine Pozrikidis, University of California, San Diego for kindly running BI calculations for further, single-drop test problems. LCN would like to acknowledge the University of Newcastle, Australia, for financial support through their Visitor Grants Scheme.

References

[1] C.A. Miller, P. Neogi, Interfacial Phenomena: Equilibrium and Dynamic Effects, Marcel Dekker, New York, 1985, pp. 1–19, 299–307.
[2] D. Myers, Surfaces, Interfaces and Colloids: Principles and Applications, VCH Publishers, Inc., New York, 1991, pp. 7–19, 87–91.
[3] A.W. Adamson, A.P. Gast, Physical Chemistry of Surfaces, sixth edn., Wiley, New York, 1997, pp. 4, 5.
[4] D.A. Edwards, H. Brenner, D.T. Wasan, Interfacial Transport Processes and Rheology, Butterworth–Heinemann, London, 1991 (Chapter 15).
[5] M.V. Berry, Phys. Educ. 6 (1971) 79.
[6] J.U. Brackbill, D.B. Kothe, C. Zemach, J. Comput. Phys. 100 (1992) 335.
[7] S.O. Unverdi, G. Tryggvason, J. Comput. Phys. 100 (1992) 25.
[8] B. Lafaurie, C. Nardone, R. Scardovelli, S. Zaleski, G. Zanetti, J. Comput. Phys. 113 (1994) 134.
[9] A.V. Coward, Y.Y. Renardy, M. Renardy, J.R. Richards, J. Comput. Phys. 132 (1997) 346.
[10] D. Gueyffier, J. Li, A. Nadim, R. Scardovelli, S. Zaleski, J. Comput. Phys. 152 (1999) 423.
[11] R. Scardovelli, S. Zaleski, Ann. Rev. Fluid Mech. 31 (1999) 567.
[12] J. Li, Y.Y. Renardy, M. Renardy, Phys. Fluids 12 (2000) 269.
[13] J.P. Morris, Int. J. Numer. Methods Fluids 33 (2000) 333.
[14] G. Tryggvason, B. Bunner, A. Esmaeeli, D. Juric, N. Al-Rawahi, W. Tauber, J. Han, S. Nas, Y.-J. Jan, J. Comput. Phys. 169 (2001) 708.
[15] Y. Renardy, M. Renardy, J. Comput. Phys. 183 (2002) 400.
[16] C. Chen, L.-S. Fan, AIChE J. 50 (2004) 288.
[17] L.C. Nitsche, U. Schaflinger, Phys. Fluids 13 (2001) 1549.
[18] A. Gray, Modern Differential Geometry of Curves and Surfaces with Mathematica, second edn., CRC Press, New York, 1998, Section 17.2.
[19] J.M. Rallison, A. Acrivos, J. Fluid Mech. 89 (1978) 191.
[20] J.M. Rallison, J. Fluid Mech. 109 (1981) 465.
[21] H.A. Stone, L.G. Leal, J. Fluid Mech. 198 (1989) 399.

[22] C. Pozrikidis, J. Fluid Mech. 210 (1990) 1.
[23] C. Pozrikidis, Boundary Integral and Singularity Methods for Linearized Viscous Flow, Cambridge University Press, New York, 1992.
[24] M. Manga, H.A. Stone, J. Fluid Mech. 256 (1993) 647.
[25] R.H. Davis, Phys. Fluids 11 (1999) 1016.
[26] C. Pozrikidis, A Practical Guide to Boundary Element Methods with the Software Library BEMLIB, Chapman & Hall/CRC Press, London/Boca Raton, 2002.
[27] G. Machu, W. Meile, L.C. Nitsche, U. Schaflinger, J. Fluid Mech. 447 (2001) 299.
[28] R.W. Hockney, J.W. Eastwood, Computer Simulation Using Particles, IOP Publishing, Philadelphia, 1988.
[29] M.P. Brenner, Phys. Fluids 11 (1999) 754.
[30] R.J. Phillips, J. Fluid Mech. 481 (2003) 77.
[31] G. Machu, Interfacial phenomena in suspensions, Ph.D Thesis, Institute of Fluid Dynamics and Heat Transfer, Technical University Graz, Austria, 2001.